Article:
Meng, T., Huang, Y., Whiteing, A. et al. (2026) Quantifying environmental impacts of cold chain interruptions using coupled CFD and LCA. Transportation Research Part D: Transport and Environment, 153. 105230. ISSN: 1361-9209

https://doi.org/10.1016/j.trd.2026.105230

Title: Quantifying environmental impacts of cold chain interruptions using coupled CFD and LCA

Graphical Abstract

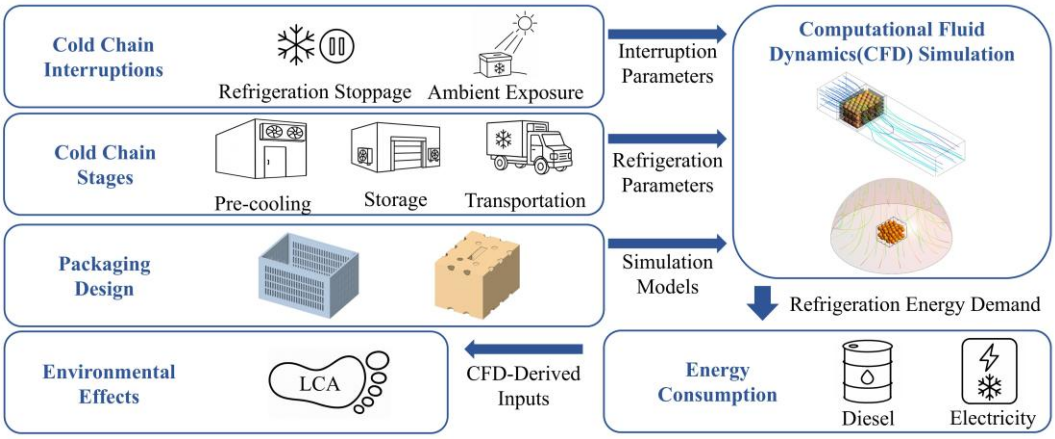

Abstract

Cold chain interruptions (CCIs) can alter energy use and emissions in cold chain logistics (FCCL), yet their impacts are often overlooked in life cycle assessment (LCA). This study integrates computational fluid dynamics (CFD) with LCA to quantify CCI-related impacts, through a gate-to- gate case study of Zigui navel oranges from precooling to cold storage at destination. CFD reconstructs temperature histories, which are converted to stage-specific refrigeration energy usage and fed into LCA to quantify environmental burdens. Two types of CCIs were evaluated: refrigeration pauses have minimal effects, while ambient exposures, especially after precooling, increase global warming potential (GWP) by up to 5.94%. Overall, refrigerated transport contributes over 85% of total GWP, with a distance–GWP slope of 0.0014 kg CO-eq/km. Replacing

diesel with B5 biodiesel (5% fatty acid methyl esters) reduces GWP by 3.95%. This CFD–LCA framework enables more accurate CCI impact assessments, supporting the design of sustainable FCCL systems.

Keywords: Cold chain interruption; Food cold chain; Life cycle assessment; Computational fluid dynamics; Energy consumption; Environmental impacts.

1 Introduction

Food Cold Chain Logistics (FCCL) refers to a temperature-controlled distribution system designed to preserve the quality, safety, and shelf life of perishable foods by maintaining thermal conditions from harvest to retail (Mustafa et al., 2024). Despite its essential role in food preservation, FCCL also contributes significantly to environmental burdens, primarily through electricity and fossil fuels, combined with refrigerant leakage, which leads to considerable direct and indirect greenhouse gas (GHG) emissions (Cui et al., 2025). It is estimated that FCCL accounts for 8%–10% of total energy use in the food supply chain and approximately 4% of global GHG emissions (UNEP and FAO, 2022). As a result, balancing preservation performance with environmental sustainability has become a critical challenge for the sustainable transition of food systems. In response, governments, industry stakeholders, and supply chain operators worldwide are increasingly committed to achieving net-zero emissions in the cold chain sector (Armstrong et al., 2025).

Among the key operational vulnerabilities in FCCL, cold chain interruption (CCI) refers to the temporary failure of temperature control caused by equipment malfunctions, power outages, transport delays, or improper handling (Skawińska and Zalewski, 2022). CCIs can lead to food quality degradation (Lohita and Srijaya, 2024), nutritional loss (Fu et al., 2024), and microbial proliferation (Haque et al., 2024), which pose serious food safety concerns. In parallel, these disruptions also cause upstream resource waste, particularly in activities such as agricultural production, harvesting, and initial processing, which lead to inefficiencies and higher resource consumption. They also intensify environmental burdens, especially when substantial energy is required to restore thermal conditions (Liu et al., 2024; Mustafa et al., 2024). While previous studies have extensively investigated the impact of temperature abuse on food quality through sensory, compositional, and microbial indicators (Fu et al., 2024; Waldhans et al., 2024), the environmental burdens associated with CCIs under realistic operating conditions have yet to be systematically quantified.

Life cycle assessment (LCA) provides a standardized framework for quantifying the environmental impacts of a product system across its full life cycle, from raw material extraction to end-of-life disposal (ISO, 2006). In the context of FCCL, LCA has been widely applied to evaluate the sustainability performance of packaging strategies (Meng et al., 2023), transportation modes (Wu et al., 2022b), and refrigeration technologies (Lin et al., 2025), offering a scientific basis for system optimization. However, most existing LCA models are built upon steady-state assumptions and rely

on generic inventory datasets that fail to reflect the operational dynamics and disruptions occurring in real cold chain systems (Corigliano and Algieri, 2024). Typically, CCIs can lead to temperature fluctuations that influence energy consumption and potentially affect product quality (Fu et al., 2024; Marques et al., 2025). These effects are highly sensitive to packaging configuration, operational parameters, and temperature history, yet are not adequately addressed in conventional LCA datasets (Wu et al., 2019a). In this context, the comparison of multiple CCIs provides a meaningful basis for assessing the environmental trade-offs involved in managing uncertainty within FCCL systems and serves to justify the use of LCA in evaluating performance variations across distinct operational disruptions.

Computational fluid dynamics (CFD) is a numerical method used to simulate fluid flow and heat transfer by solving the governing equations of thermodynamics and fluid mechanics (Ferziger et al., 2019). Its primary strength lies in delivering high-resolution spatial and temporal data, making it particularly suitable for systems with complex airflow and thermal dynamics (Daniel et al., 2024). In FCCL applications, CFD enables the reconstruction of dynamic temperature trajectories (Chen et al., 2024), providing a physically grounded basis for estimating transient refrigeration loads and the associated environmental burdens (Daniel et al., 2024; Wu et al., 2019a, 2018). However, these thermal simulations have rarely been linked with life cycle inventory models, limiting their capacity to inform system-level environmental assessments under fluctuating operating conditions (Szpicer et al., 2023). To address this gap, this study develops an

integrated CFD–LCA framework to quantify the environmental impacts of temperature fluctuations during FCCL. The proposed approach focuses on estimating transient refrigeration energy consumption and the resulting environmental burdens, offering a dynamic and physically informed basis for evaluating the sustainability performance of FCCL systems.

To assess the sustainability consequences of CCIs, this study establishes a systematic methodology that couples high-resolution thermal simulations with environmental impact evaluation. Series of CFD models are constructed to simulate heat transfer dynamics and transient temperature evolution under both stable and interrupted FCCL scenarios. The resulting temperature histories are used to estimate refrigeration energy consumption, which is then integrated into an LCA model to quantify the environmental impacts of different CCI scenarios. The FCCL of Zigui navel oranges from origin to Beijing serves as a representative case due to their summer ripening characteristics, high perishability, and concentrated origin with broad market distribution across China's cold chain logistics. The integrated CFD–LCA framework enables dynamic and spatially resolved environmental assessment, contributing both methodological advancement and practical insights for the design and optimization of sustainable FCCL systems.

2 Methods

2.1 Cold Chain Stages and CCIs

The modeled FCCL system covers the postharvest logistics of navel oranges from the production region in Hubei Province to a retail cold storage facility in Beijing. This system includes four stages:

(1) Precooling: Following harvest and sorting, oranges are rapidly cooled using forced-air systems to remove field heat. During this phase, fruits are packed in reusable plastic containers (RPCs), each holding 128 standard oranges (**Figure 1a**). Due to their excellent ventilation performance and reusability, RPCs are widely used during precooling to enhance airflow circulation and accelerate core temperature reduction. (Gruyters et al., 2019).

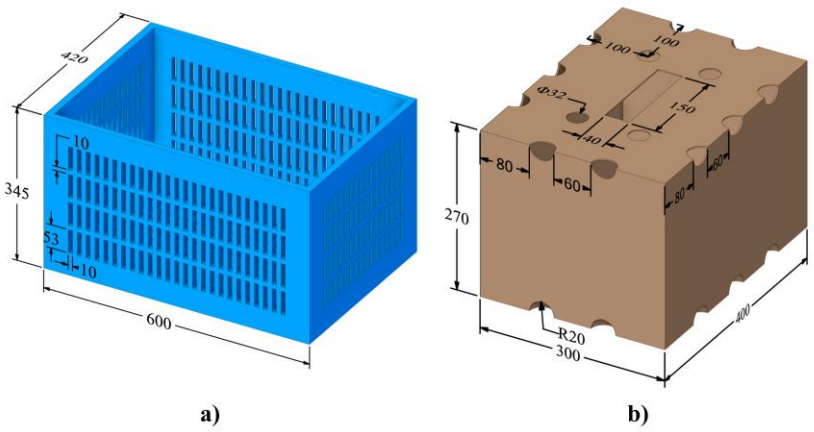

Figure 1 Packaging used in the FCCL system (unit: mm): a) RPC; b) Supervent CCB(Wu et al., 2018).

(2) Initial Storage: After precooling, oranges are placed in a cold storage facility at the origin. Prior to storage, fruits are repacked into Supervent corrugated cardboard boxes (CCBs), with 64 fruits per box (**Figure 1b**). This packaging configuration

enhances airflow, reduces intra-box temperature gradients, and improves cooling efficiency (Wu et al., 2019b).

(3) Refrigerated Transportation: The packaged oranges are then transported to a cold storage in Beijing using diesel-powered, Euro V-compliant refrigerated trucks charged with 1,1,1,2-Tetrafluoroethane (R134a) refrigerant. Each truck operates with a payload of 3.5–7.5 tons over a transport distance of 1360 km from Zigui.

(4) Final Storage: Upon arrival, the oranges are stored in the retail-distribution cold warehouse pending dispatch for sale.

The packaging types, refrigeration setpoints, and durations associated with each FCCL phase are summarized in **Table 1**.

Table 1 Packaging types, refrigeration temperatures, and durations across FCCL stages.

Cold Chain Phases	Packaging Boxes	Temperature (°C)	Duration (days)
Pre-cooling	RPC	3	3
Initial Storage	CCB	3	5
Transportation	CCB	-1	2
Final Storage	CCB	4	10

*Note: During transportation, due to mixed loading with other products, the target temperature is lower than the optimal storage temperature for oranges. However, the oranges do not freeze, as the dissolved sugars and other solutes depress their freezing point (Tian et al., 2022).

CCIs can arise not only within individual FCCL phases but also during the transitional handling processes that connect them. To facilitate systematic environmental evaluation, CCIs are categorized into two representative types in this study:

(1) Refrigeration Pauses: These interruptions occur during any FCCL phase when cooling is suspended due to equipment failure or power outages. Although the products remain within insulated environments (e.g., refrigerated warehouses or vehicles), the lack of active refrigeration can lead to gradual temperature increases.

(2) Ambient Exposure: This type of interruption occurs during inter-phase handling operations, where products are temporarily exposed to ambient conditions during loading, unloading, or transfer. In some cases, delays or mishandling may result in prolonged exposure. For this study, the ambient temperature is set at 21 °C, reflecting the average conditions along the transport route in May.

The seven specific CCI scenarios examined in this study are defined in **Table 2,** with their positions along the cold chain illustrated in **Figure 2**.

Table 2 Classification and definitions of CCI scenarios.

Category	CCI Scenarios and Abbreviations
Refrigeration Pauses	Interruption in Pre-cooling (IPC)
	Interruption in Initial Storage (IIS)

	Interruption in Cold Chain Transportation (ICT)
	Interruption in Final Storage (IFS)
	Ambient Exposure after Pre-cooling (AEPC)
Ambient Exposure	Ambient Exposure after Initial Storage (AEIS)
	Ambient Exposure after Cold Chain Transportation (AECT)

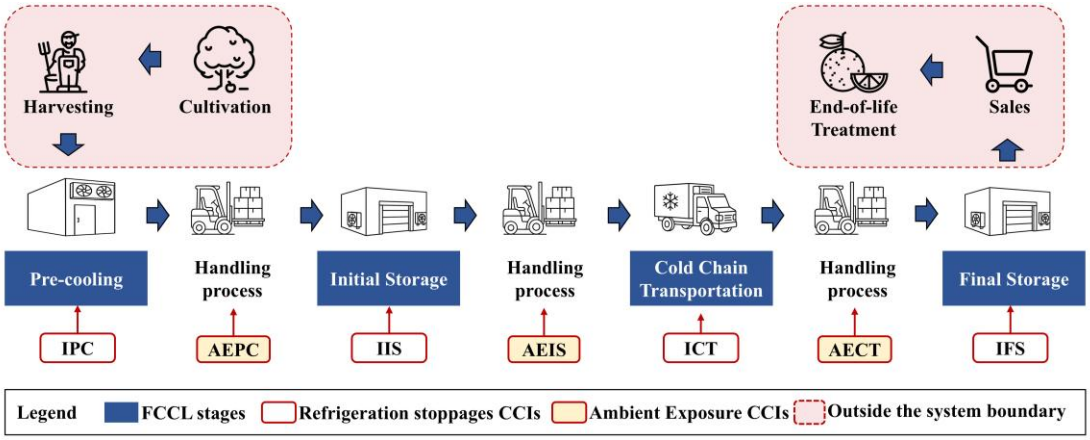

Figure 2 Cold chain stages and handling processes where two types of CCIs may occur.

In practice, CCIs are typically short-lived, as operators strive to minimize disruptions through contingency protocols and rapid operational responses. Reflecting this operational reality, all CCIs in this study are modeled with limited durations ranging from 1 to 3 hours. These durations align with observed delays in commercial cold chains and enable consistent comparison across interruption cases (Conradie et al., 2022; Owoyemi et al., 2023).

2.2 CFD modeling

To quantify the impact of CCIs on refrigeration energy demand, CFD was employed to simulate heat transfer and temperature evolution throughout the FCCL process. Two types of simulation models were developed to represent distinct interruption mechanisms.

For uninterrupted operation and refrigeration pause CCIs, three CFD models were developed to represent the FCCL phases: precooling (**Figure 3a**), refrigerated transportation (**Figure 3b**), and cold storage (encompassing both initial and final storage) (**Figure 3c**). In refrigeration pause simulations, cold airflow was disabled while thermal insulation was retained, allowing for the passive heat gain experienced during system shutdowns. All geometries were based on real RPC and Supervent CCB packaging, ensuring fidelity in airflow and heat transfer modeling. To mitigate boundary effects and enhance numerical stability, extended inlet and outlet regions were incorporated into the air domain upstream and downstream of the product load.

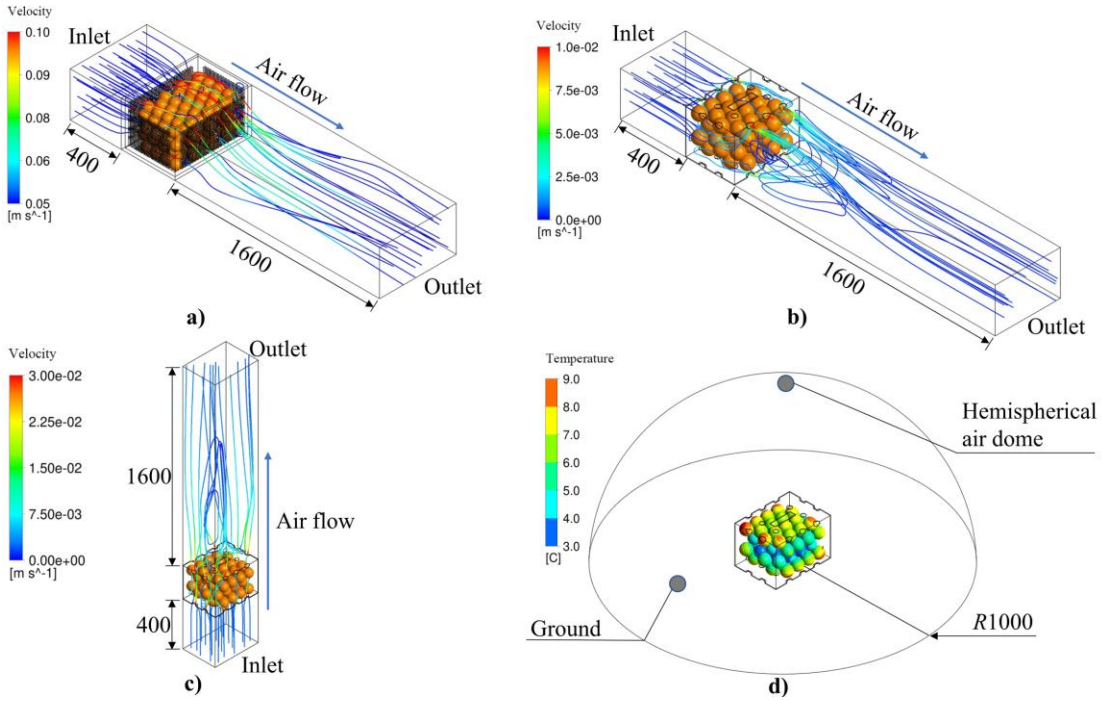

Figure 3 CFD geometry configurations for FCCL and CCIs: a) precooling, b) refrigerated transportation, c) cold storage, and d) ambient exposure (unit: mm).

To simulate ambient exposure CCIs during handling processes, a dedicated CFD model was constructed using a hemispherical air domain, with a fully loaded CCB placed on a flat surface at ambient temperature (21 °C) (**Figure 3d**). This geometric configuration was selected to more accurately replicate open-air conditions by allowing unobstructed natural convection around the carton. The hemispherical domain provides sufficient space for airflow development and minimizes artificial boundary interference, which is essential for capturing realistic thermal interactions between the product and the surrounding environment (Baïri, 2014).

In all cases, CFD simulations resolved the coupled airflow and heat transfer dynamics, yielding transient temperature fields as outputs. These results formed the

physical basis for refrigeration energy estimation and subsequent environmental impact evaluation. For each cold chain scenario and CCI event, the temperature outputs from different CFD models were temporally linked, ensuring continuity across phases and enabling dynamic tracking of fruit thermal history throughout the FCCL process. The specific configurations of mesh generation, solver settings, turbulence modeling, and thermophysical properties are documented in **Supplementary Information A**.

2.3 Energy Use Estimation

To quantify refrigeration energy demand across different FCCL stages and CCI scenarios, temperature–time profiles generated from CFD simulations were used as dynamic thermal inputs. For each FCCL stage, energy use was calculated by separating the rapid cooling and temperature holding periods, based on the Seven-Eighths Cooling Time (SECT) criterion. SECT is defined as the time when the core temperature of the fruit has decreased by seven-eighths of the initial temperature difference and is commonly used to delineate the end of the rapid cooling phase in FCCL (Wang et al., 2022). This stage-level distinction allows both cooling and holding periods to be identified within any FCCL stages, depending on the temperature trajectory.

2.3.1 Energy Use in Cooling Phase

During the cooling phase (pre-SECT), rapid temperature reduction is achieved through convective heat exchange between warm fruit and refrigerated air. Electrical

energy consumption in this phase depends on system performance, packaging airflow resistance, and fruit thermophysical properties. To convert fruit cooling loads to actual energy use, an Energy Coefficient (EC) is applied, defined as the amount of heat removed from fruit per unit of electricity consumed:

$$EC = \frac{m \cdot c_p \cdot (T_i - T_f)}{E_e \cdot c} \quad (1)$$

where: m is the fruit mass (kg), c_p is the specific heat capacity (kJ·kg^{-1}·K^{-1}), T_i and T_f are the initial and final core temperatures (°C), E_e is the electricity consumed (kWh), c is the conversion factor (3600 kJ·kWh^{-1}).

Following existing literature (J. F. Thompson et al., 2010; Wu et al., 2019a), the EC for Supervent CCBs was set to 0.41 during precooling and transportation, and 0.40 during storage. For RPCs, CFD simulations yielded an EC of 0.40, reflecting their enhanced ventilation performance and reduced airflow resistance.

The cumulative cooling energy per kilogram of fruit was calculated by integrating the temperature drop over discrete time steps n until SECT is reached:

$$Q_{cooling/kg} = \sum_{n=1}^{N} \frac{c_p \cdot \Delta T_n}{EC \cdot c} \quad (2)$$

where ΔT_n is the core temperature drop at step n, and N is the total number of steps until SECT.

2.3.2 Energy Use in Holding Phase

Following SECT, the holding phase involves maintaining fruit at low temperature while countering external heat gain. Energy use in this phase is a function of ambient temperature, enclosure insulation, and thermal leakage. Based on empirical measurements of 20-foot refrigerated containers (TEUs) (Fitzgerald et al., 2011; Stoessel et al., 2012), the average power requirement can be estimated as:

$$P_{TEU} = 0.0696T_e + 0.9406 \tag{3}$$

Where: P_{TEU} is the average power per container (kW), and T_e is the external temperature (°C).

Assuming a load capacity of 9769 kg (9 pallets × 80 boxes per pallet), the per-kilogram energy use during holding over time t (hours) is:

$$Q_{holding/kg} = P_{TEU} \cdot \mathrm{t}/9769 \tag{4}$$

The total refrigeration energy demand per kilogram of fruit in each cold chain stage or interruption scenario is then:

$$Q_{total/kg} = Q_{\mathrm{cooling/kg}} + Q_{\mathrm{holding/kg}} \tag{5}$$

2.4 Integration of CFD and LCA Modeling

CFD–LCA integration enables quantitative linkage between thermal dynamics and environmental impacts under FCCL scenarios. Transient temperature fields obtained from CFD simulations (section 2.2) are translated into refrigeration energy demand

using the EC method, which accounts for both active cooling and thermal loads (Section 2.3). These energy estimates, together with material and transport inventories, form the basis of a process-based LCI model used for assessing environmental impacts (see Graphical Abstract). Notably, CFD results do not yield environmental indicators directly, but provide the thermal inputs necessary for accurately estimating electricity consumption in each FCCL stage.

2.4.1 Goal and System Boundary Definition

To enable quantitative evaluation, the analysis adopts a functional unit of 1 kg of Zigui navel oranges delivered to the retailer in compliance with the "First-Grade Fruit" quality standard (SAC, 2008), covering the cold chain from postharvest precooling to final storage.

A gate-to-gate system boundary is adopted, covering the stages from when graded oranges enter the precooling process to the completion of final cold storage (**Figure 4**). This boundary is consistent with the FCCL phase definitions in Section 2.1 and includes the associated use of packaging systems. Upstream agricultural production (such as cultivation and harvesting) and downstream consumption and end of life treatment of packages are excluded, as they are beyond the scope of the FCCL framework applied in this study. Additionally, fruit quality modeling and shelf life estimation (**Supplementary Information B**) confirm that the oranges meet acceptable

commercial standards under all modeled FCCL scenarios, ensuring comparability across LCA cases.

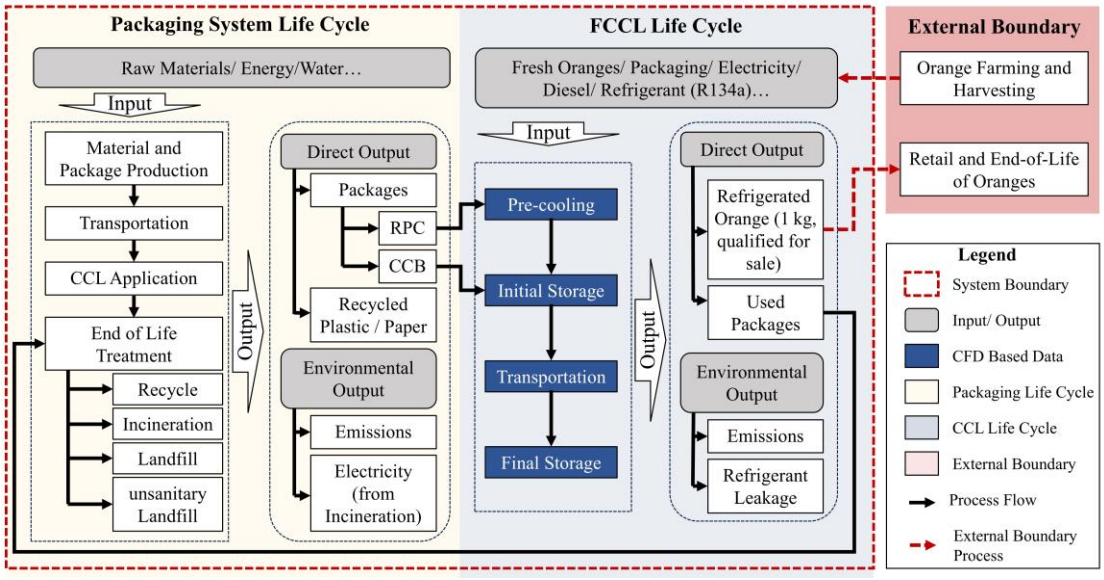

Figure 4 System Boundary and Life Cycle Structure of the Packaging and FCCL Systems.

In this study, assumptions were made to ensure the transparency and accuracy of the analysis. First, it is assumed that even if the oranges experience a CCI, their quality will not degrade to a level where they are no longer suitable for sale. The modeling of orange quality is detailed in **Supplementary Information B**. Second, for the two types of CCIs, the duration of the interruptions is assumed to range from 1 to 3 hours. For ambient exposure, the external environment is assumed to remain stable at 21°C (Section 2.1). Third, regarding refrigeration facilities, it is assumed that their cooling efficiency remains constant (Section 2.3) and the annual refrigerant leakage rate is assumed to be 10% (Section 2.4.4). Fourth, assumptions regarding the service life of packaging boxes and the end-of-life treatment ratio are based on supplier data and

relevant literature (Section 2.4.2). Further details on the CFD modeling process and associated assumptions can be found in **Supplementary Information A**.

2.4.2 Packaging

Separate LCIs were established for two packaging types: RPCs and CCBs, serving as environmental inputs for the packaging stage. In the precooling phase, fruits are cooled using RPCs composed of polypropylene (PP, 70%) and high-density polyethylene (HDPE, 30%), weighing 1.8 kg per unit.(Sasaki et al., 2021) RPCs typically do not have a mandatory end-of-life (EOL) threshold, but a service life of 700 cycles is assumed based on a six-year performance guarantee provided by the manufacturer. This value falls within the range reported in existing LCA studies, where typical lifespans vary from 300 to 1260 uses depending on handling intensity and reuse conditions (Ceballos-Santos et al., 2024; Goellner and Sparrow, 2014). To assess the influence of life-span assumptions, sensitivity analysis on RPC reuse cycles is conducted in Section 3.1. Production inputs (materials, electricity, water) are sourced from ecoinvent and adapted using China-specific background data.

For later FCCL phases, fruits are stacked in Supervent CCBs (0.37 kg each), made primarily of recycled paper (95%) (Duan et al., 2019). Given limited recovery in practice, a 49% recycling rate is assumed (Ministry of Commerce of People's Republic of China, 2021), with the remainder distributed across incineration (16%), landfill (32%), and unsanitary landfill (3%), based on national statistics (Duan et al., 2019).

LCI data are normalized to the unit packaging level and subsequently converted to emissions per kilogram of transported fruit according to container capacity. Detailed inventory flows and emission factors are summarized in **Table 3**.

Table 3 LCI of the two packaging boxes (RPC and CCB).

Carrier Type	Flow/ Process	Type	Quantity	Unit
RPC	**Input**			
	Polypropylene, PP, granulate	Material	1.26	kg
	Polyethylene, high density, granulate	Material	0.54	kg
	Electricity, medium voltage	Energy	3	MJ
	Tap water	Material	2	L
	Output			
	RPC box (PP+HDPE), final product	Product	1	piece
	Waste polyethylene terephthalate, for recycling	Waste	0.02	kg
Supervent CCB	**Input**			
	Corrugated board	Material	0.3708	kg
	Starch-based adhesive	Material	0.005	kg
	Electricity, medium voltage	Energy	0.4	MJ
	Tap water	Material	0.1	L
	Heat, from steam	Energy	0.2	MJ
	Ethylene vinyl acetate copolymer	Material	0.02	kg

	Output			
	CCB box, final product	Product	1	piece
	waste paper	Waste	0.02	kg

Data source: Material composition data were obtained directly from packaging suppliers. The manufacturing processes and input flows were modeled using ecoinvent v3.8 datasets and subsequently adapted to reflect Chinese industrial conditions, based on localized background data and published literature (Gao et al., 2025; Guo et al., 2022; Meng et al., 2023).

2.4.3 FCCL phases

Electricity-based centralized refrigeration systems are employed in both precooling and cold storage phases. The corresponding energy demand under each CCI scenario was estimated using CFD simulations, coupled with the EC method as described in Section 2.3. These outputs provide stage-specific electricity consumption profiles, and are directly used as inventory inputs, which avoid reliance on generalized emission factors or steady-state assumptions.

Refrigerated transport is disaggregated into two functionally distinct subsystems: (1) the traction unit powered by a diesel engine, and (2) an independent transport refrigeration unit (TRU) powered by a dedicated auxiliary diesel generator. This structural decomposition follows practices established in prior LCA studies (Fabris et al., 2022; Shi et al., 2015; Wu et al., 2022a), recognizing the distinct energy profiles and emission intensities of each subsystem.

Traction-related emissions are estimated using ecoinvent datasets for medium-duty diesel trucks, adjusted to reflect actual route distances and vehicle specifications. TRU-related energy demand is derived from CFD outputs and converted to electricity use per kilogram of fruit using the EC method. To model the upstream emissions from onboard electricity generation, the ecoinvent process "diesel, burned in diesel-electric generating set, 18.5 kW" is employed, assuming a thermal efficiency of 35.1% in line with established literature (Shi et al., 2015; Tassou et al., 2009). This dataset captures diesel combustion, conversion losses, and generator infrastructure burdens.

2.4.4 Refrigerant leakage

R134a is currently the dominant refrigerant used in FCCL in China, having replaced earlier ozone-depleting substances such as chlorofluorocarbons (CFCs, e.g., R12) and hydrochlorofluorocarbons (HCFCs, e.g., R22), which have been largely phased out under the Montreal Protocol (Gao et al., 2021). As a hydrofluorocarbon (HFC), R134a contains no chlorine or bromine atoms and therefore does not contribute to stratospheric ozone depletion (IPCC, 2021). However, it has a 100-year GWP of 1430 (IPCC, 2021). Thus, even minor leakage can still result in significant environmental impacts.

Stage-specific refrigerant emissions were estimated based on equipment charge quantities, occupancy durations (**Table 1**), and fruit-handling capacities per batch. The precooling chamber, seasonally operated with 4.0 kg of R134a, handles 9769 kg of fruit

per batch. Initial cold storage facilities contain 20 kg of R134a and accommodate 97,690 kg per batch. Transport is performed using a TRU-equipped vehicle charged with 3.0 kg of R134a and loaded with 9769 kg of fruit. All input values were obtained through field surveys and equipment documentation.

A uniform annual leakage rate of 10% was assumed for all systems, consistent with values reported for commercial cold storage and refrigerated trucks (IPCC, 2006; Stellingwerf et al., 2018; Tassou et al., 2009; Wu et al., 2022b). Emissions per kilogram of fruit were derived by scaling the annual leakage to each stage's operation time and dividing by batch throughput. The resulting leakage intensities are 3.37×10^{-7} kg R134a/kg for precooling, 2.81×10^{-7}kg R134a/kg for initial cold storage, 1.68×10^{-7}kg R134a/kg for transport, and 5.62×10^{-7} kg R134a/kg for final cold storage.

All inventory flows were normalized to the defined functional unit of 1 kg of oranges and integrated into a process-based LCA model. **Table 4** summarizes the resulting baseline inventory without CCIs. Under CCI scenarios, electricity and diesel consumption may vary due to altered thermal loads, making this baseline a reference for comparative assessments.

Table 4 LCI of the FCCL system under baseline (no interruption) conditions, normalized to 1 kg of oranges.

Stages	Flow/ Process	Type	Direction	Quantity	Unit
Precooling	RPC	Packaging	Input	5.3E-05	piece

	Navel Orange (ambient)	Product	Input	1.0E+00	kg
	Electricity, medium voltage	Energy	Input	8.4E-02	kWh
	R134a	Refrigerant	Output	3.4E-07	kg
Initial storage	CCB	Packaging	Input	7.4E-02	piece
	Electricity, medium voltage	Energy	Input	8.0E-05	kWh
	R134a	Refrigerant	Output	2.9E-07	kg
Transportation	lorry 3.5-7.5t, EURO 4 (for traction)	Transportation	Input	1.4E+03	kgkm
	Diesel-electric generating set, 18.5kW (for TRU)	Energy	Input	9.8E-03	kWh
	R134a	Refrigerant	Output	1.7E-07	kg
Final Storage	Electricity, medium voltage	Energy	Input	1.6E-04	kWh
	R134a	Refrigerant	Output	5.6E-07	kg
EOL: RPC	Waste plastic, municipal incineration	Waste treatment	Output	1.9E-05	kg
	Waste plastic, for recycling	Waste treatment	Output	7.6E-05	kg
EOL: CCB	Waste paper, core board production	Waste treatment	Output	1.3E-02	kg
	Waste paper, municipal incineration	Waste treatment	Output	4.1E-03	kg

	Waste paperboard, sanitary landfill	Waste treatment	Output	8.3E-03	kg
	Waste paperboard, unsanitary landfill	Waste treatment	Output	7.7E-04	kg
Final Product	Navel Orange (Chilled)	Product	Output	1.0E+00	kg

Data source: Energy consumption values are based on CFD-derived simulations. Transport and packaging flows reflect assumptions and system configurations established in this study. Waste treatment pathways and allocation ratios are adapted from ecoinvent v3.8 datasets and modified to reflect current waste management practices in China (Section 2.4.2).

Environmental impacts were assessed using ReCiPe 2016 at the midpoint level, which provides comprehensive coverage across multiple impact categories (Huijbregts et al., 2017). In addition to global warming potential (GWP), five indicators were selected to reflect key stressors in FCCL: human non-carcinogenic toxicity (HnCTP), fossil resource scarcity (FRSP), ozone formation for human health (OFP(HH)), acidification (AP), and particulate matter formation (PMFP). These indicators were chosen based on their relevance to refrigeration energy use, packaging materials, refrigerant leakage, and transport emissions. Specifically, HnCTP captures chemical exposure risks, FRSP reflects fossil fuel and plastic dependence, OFP(HH) and PMFP address emissions from diesel combustion, and AP represents acidifying air pollutants. Together, they complement GWP and provide a more complete picture of the environmental footprint of FCCL systems.

3 Results and discussion

3.1 Environmental performance of the uninterrupted scenario

The baseline scenario represents a fully functional FCCL without interruption, yielding a total GWP of 0.881 kg CO_2-eq per kilogram of orange. As shown in **Figure 5**, vehicle traction is the dominant contributor (86.3% of the total), followed by packaging and precooling. This finding aligns closely with previous studies (Bin et al., 2022), confirming that our CFD-LCA method produces results consistent with traditional LCA approaches in the uninterrupted FCCL, thus validating the robustness and comparability of our methodology. Other processes, including cold storage, TRU operation, and refrigerant leakage, have marginal impacts as shown in **Table 5** and **Figure 6**.

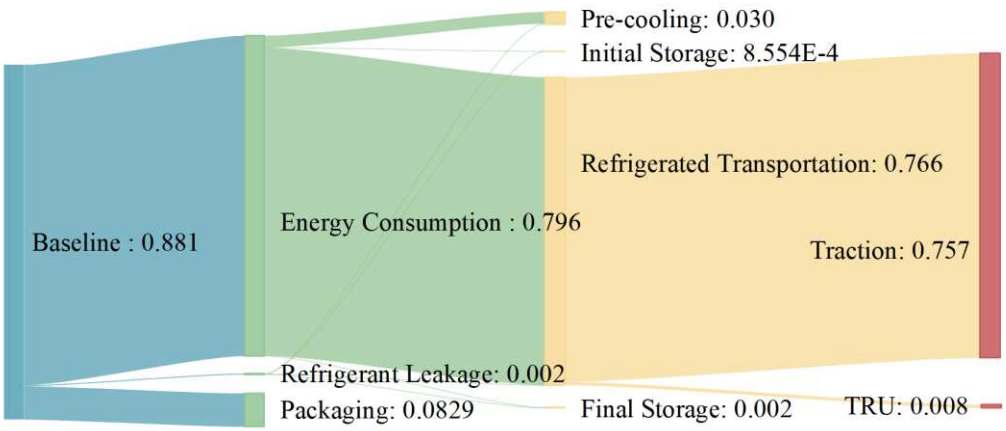

Figure 5 Contribution of GHG emissions under the baseline scenario (per kg of orange).

Table 5 Environmental impact results under the baseline scenario (per kg of orange).

FCCL Component	GWP	HnCTP	FRSP	OFP(HH)	AP	PMFP

Unit	kg CO_2-eq to air	kg 1,4-DCB	kg oil eq	kg NO_x-eq to air	kg SO_2 eq	kg $PM_{2.5}$-eq to air
Packaging	8.3E-02	5.5E-02	1.7E-02	1.6E-04	1.7E-04	2.7E-05
Refrigerant leakage	2.5E-03	1.3E-07	0.0E+00	0.0E+00	0.0E+00	0.0E+00
Pre-cooling	2.9E-02	1.4E-02	5.7E-03	8.1E-05	1.0E-04	4.5E-05
Initial Storage	4.2E-04	1.9E-04	8.2E-05	1.2E-06	1.4E-06	6.4E-07
Traction	7.6E-01	6.9E-01	2.5E-01	2.1E-03	1.9E-03	8.3E-04
TRU	8.5E-03	2.7E-03	2.6E-03	1.3E-04	6.2E-05	3.5E-05
Final Storage	8.4E-04	3.9E-04	1.6E-04	2.3E-06	2.9E-06	1.3E-06
Total	8.8E-01	7.6E-01	2.7E-01	2.5E-03	2.2E-03	9.3E-04

A broadly consistent contribution pattern is observed across all selected midpoint indicators, with variations reflecting the distinct emission profiles of each category (**Figure 6**). Traction remains the dominant source of environmental burden, contributing between 85.0% and 90.8% of the total impacts. Packaging ranks second, with shares ranging from 2.9% to 9.4%, followed by precooling (1.8%–4.8%) and the TRU (0.4%–5.2%). Cold storage and refrigerant leakage consistently contribute less than 0.3% in all categories. Notably, TRU-related impacts are slightly more pronounced under PMFP and OFP(HH) due to diesel combustion emissions.

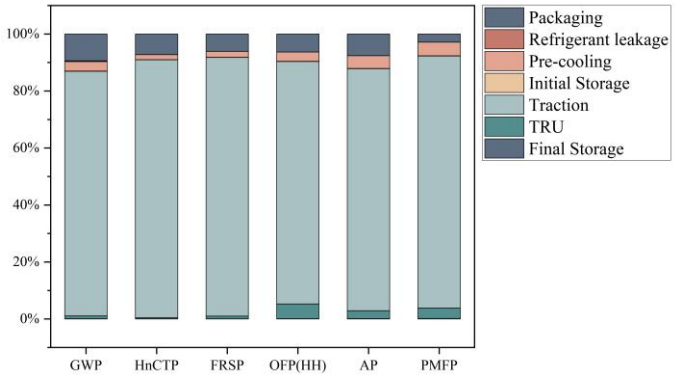

Figure 6 Relative contributions of FCCL components to six midpoint impact categories under the baseline scenario.

This impact distribution reflects the energy intensity and residence time of each cold chain phase. Vehicle traction dominates due to long-distance diesel consumption (Neittaanmäki et al., 2024). Packaging ranks second, primarily due to the high material demand of RPCs, which are PP and HDPE, and the end-of-life burdens associated with single-use CCBs (Meng et al., 2023). Precooling, though temporally brief, requires high power to remove field heat rapidly, making it the largest of the FCCL cooling phases (Bin et al., 2022). The TRU, while handling smaller thermal loads, operates continuously via an auxiliary diesel engine, producing measurable impacts in all categories (Wu et al., 2022a). Cold storage has low environmental intensity, as it primarily involves temperature maintenance with low energy input over moderate durations (Bin et al., 2022). Although refrigerant leakage is minor in absolute terms, it serves as a relevant indicator of system integrity and presents an opportunity for further optimization.

3.2 Environmental performance under CCIs

3.2.1 Refrigeration Pauses

1-3 hours refrigeration pauses (IPC, IIS, ICT, and IFS) resulted in limited variations across all mid-point environmental indicators, assuming the FCCL facility is well-insulated to minimize heat exchange during the interruption. This condition helps maintain stable thermal conditions and reduces the need for additional energy consumption. Existing research supports the importance of temperature stability in reducing FCCL's environmental impacts (Rai, 2019). Studies have shown that maintaining stable temperatures minimizes recovery cooling, reducing energy use and emissions (Cui et al., 2025; Dong et al., 2020; Marchi et al., 2022). These findings further support our conclusion that refrigeration pauses have limited environmental impacts by maintaining temperature stability.

Among these, the IFS scenario exhibited the highest system resilience, with changes in GWP, HnCTP, FRSP, OFP(HH), AP, and PMFP all remaining below 3.81×10^{-5}%. This is because, following transportation, the fruit core temperature is already below the target for final storage. The refrigeration system operates in a low energy holding mode, requiring minimal active cooling during the interruption period.

In contrast, IPC and IIS led to modest increases in environmental burdens, with IIS consistently producing higher values than IPC. For example, PMFP increased by 0.011% in IPC and by 0.023% in IIS, while AP rose by 0.009% and 0.021%,

respectively (**Table 6** and **Figure 7**). These results suggest that interruptions occurring earlier in the FCCL are more environmentally sensitive, as the system has not yet reached thermal equilibrium and therefore requires greater energy input for recovery.

Table 6 Relative changes in midpoint impact indicators under 3-hour CCI scenarios compared to the baseline.

CCIs	GWP	HnCTP	FRSP	OFP-HH	AP	PMFP
IPC	0.006%	0.003%	0.004%	0.009%	0.009%	0.011%
IIS	0.013%	0.007%	0.009%	0.021%	0.021%	0.023%
ICT	-0.026%	-0.010%	-0.026%	-0.139%	-0.074%	-0.100%
IFS	0.000%	0.000%	0.000%	0.000%	0.000%	0.000%
AEPC	5.938%	3.109%	3.852%	7.343%	8.511%	9.403%
AEIS	0.481%	0.180%	0.477%	2.595%	1.381%	1.857%
AECT	0.001%	0.001%	0.001%	0.001%	0.002%	0.002%

Data source: Energy consumption values are based on CFD-derived simulations. Transport and packaging flows reflect assumptions and system configurations established in this study. Waste treatment pathways and allocation ratios are adapted from ecoinvent v3.8 datasets and modified to reflect current waste management practices in China (Section 2.4.2).

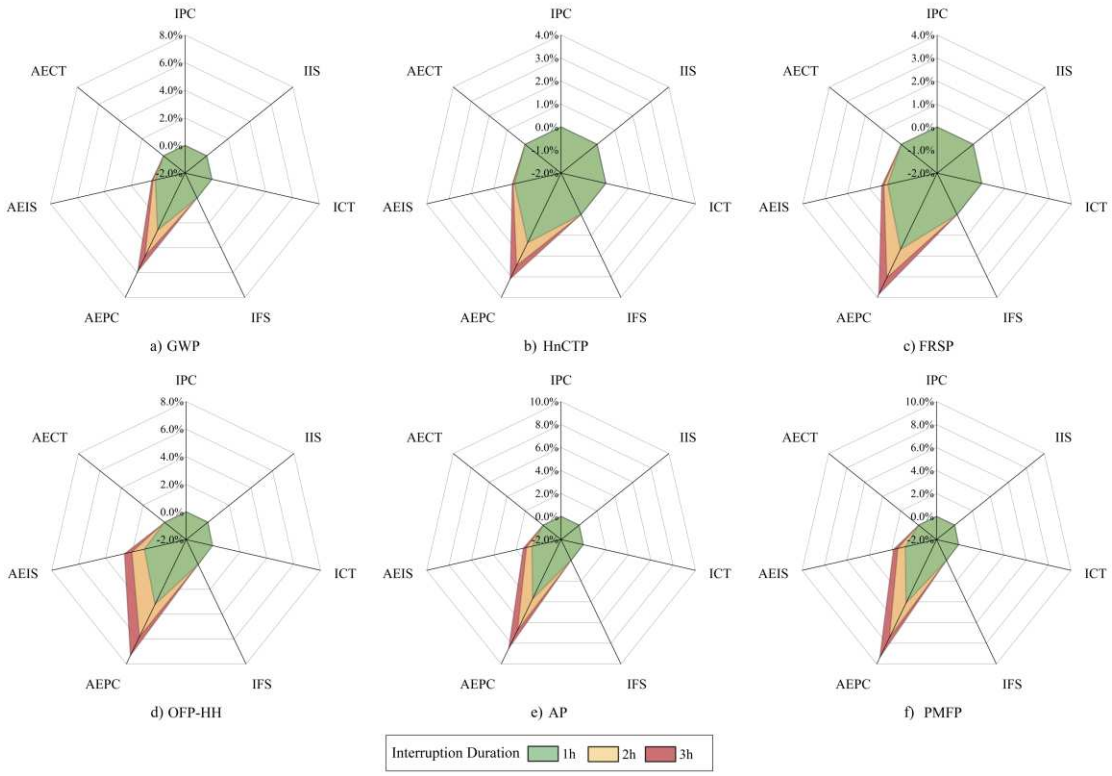

Figure 7 Relative changes in environmental midpoint indicators under different CCI scenarios and durations. (For interpretation of the references to colour in this figure legend, the reader is referred to the web version of this article.)

Stage-level decomposition of GWP (**Figure 8**) reveals that increases in IPC and IIS are primarily attributable to the initial storage phase. In IPC, emissions from this stage rose from 4.43×10^{-4} to 4.69×10^{-4} kg CO_2-eq as the interruption duration extended from 1 to 3 hours. In IIS, the corresponding increase was from 4.45×10^{-4} to 5.24×10^{-4} kg CO_2-eq. Minor increases were also observed in cold chain transportation, while other stages remained unchanged. As a result, the total GWP in IPC increased from 0.003% to 0.006% over the 1–3 h range.

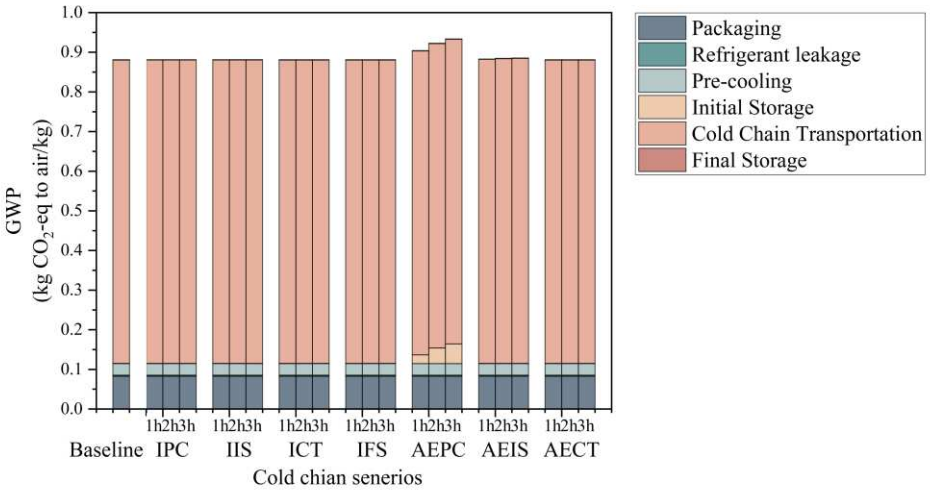

Figure 8 GWP contributions of FCCL stages under baseline and 3-hour CCI scenarios.

In contrast to IPC and IIS, the ICT scenario was associated with consistent reductions across all indicators. For a 3-hour interruption, GWP and FRSP decreased by 0.026%, and OFP(HH) by 0.139%. These reductions originated exclusively from the refrigerated transportation stage. During the interruption, the TRU was temporarily shut down under relatively stable thermal conditions, reducing diesel consumption without triggering rebound cooling. Since the fruit core temperature remained stable, no compensatory energy input was required after the interruption, resulting in a net decrease in emissions.

3.2.2 Ambient Exposure

Compared to refrigeration pauses CCIs, ambient exposure CCIs (AEPC, AEIS, AECT) resulted in substantially greater environmental impacts across all midpoint indicators. While refrigeration pauses CCIs typically caused variations below 0.01%,

or even reductions (e.g., −0.026% GWP under 3-hour ICT), ambient exposure CCIs led to multi-percentage increases, especially with prolonged durations (**Table 6** and **Figure 8**). This contrast reflects the importance of thermal boundaries: sealed environments limit heat gain through insulation, whereas ambient exposure introduces direct thermal loads requiring additional energy for compensation.

AEPC generated the most severe impact. GWP increased from 8.81×10^{-1} to 9.34×10^{-1} kg CO_2-eq as exposure time rose from 1 to 3 hours, representing a 5.94% increase (**Figure 7**). This was driven primarily by the Initial Storage phase, where emissions rose from 4.21×10^{-4} to 4.97×10^{-2} kg CO_2-eq, nearly two orders of magnitude higher than in refrigeration pauses CCIs. The increase reflects re-cooling demands after significant heat absorption during exposure. Post-precooling, fruit temperature rises quickly due to low thermal mass and high surface-area-to-volume ratio, requiring more intensive cooling in subsequent storage.

This upstream disturbance also affects refrigerated transportation. Products enter transit above the target temperature, extending TRU operation and increasing emissions by 3.01×10^{-3} kg CO_2-eq. These results highlight the importance of uninterrupted thermal control during pre-loading. Even brief exposure can undermine previous cooling and increase downstream energy demand. Mitigation strategies, such as shaded transfer areas or temperature-controlled docks, are therefore essential.

AEIS caused moderate but consistent increases. GWP rose by 0.21% to 0.48% over 1 to 3 hours, mainly due to increased fuel use in transport (from 7.65×10^{-1} to 7.70×10^{-1} kg CO_2-eq) as the TRU compensates for elevated starting temperatures. Other stages remained stable, indicating that the thermal impact is localized but extends into the transport phase.

AECT produced minimal changes. GWP increased by only 0.001%, with no significant variation except a slight rise in Final Storage emissions (from 8.42×10^{-4} to 8.54×10^{-4} kg CO_2-eq). The short exposure time and modest temperature difference allowed rapid recovery without major energy penalties.

Across all indicators, environmental burdens increased with exposure duration (**Figure 8**). For GWP, AEPC showed a 2.60% increase after 1 hour, rising to 4.69% and 5.94% for 2 and 3 hours, respectively. Similar trends were observed for HnCTP, FRSP, OFP(HH), AP, and PMFP.

Impact severity also varies with timing. AEPC caused the largest increases by disrupting early thermal stability, which amplified energy use in storage and transport. AEIS produced moderate effects, primarily in transport. AECT had negligible impact, suggesting that late-stage exposures are easier to correct. These findings emphasize that both the duration and timing of ambient exposure are key determinants of cold chain environmental performance.

In this study, ambient exposure represents an extreme form of cold chain interruption. Similarly, the opening and closing of doors in refrigerated trucks and warehouses can also disrupt the cold chain. The frequency and duration of these interruptions significantly impact the energy consumption of refrigeration systems and their environmental effects. More frequent door openings and lower set temperatures lead to higher environmental impacts due to increased FCCL (Lin et al., 2025). This aligns with the study's conclusion that greater re-cooling demand on refrigeration equipment exacerbates the environmental burden.

3.3 Sensitivity Analysis

The life cycle results above are based on fixed assumptions such as transport distance, packaging reuse lifespan, and the energy efficiency of the TRU generator. To assess the robustness of these results and identify critical parameters, we conducted both deterministic sensitivity analyses and stochastic uncertainty simulations.

A parametric sensitivity analysis was first performed on two key variables: transport distance and reusable packaging lifespan. Given that traction emissions dominate GWP, ±20% variations in transport distance were simulated by adjusting average speed under a fixed TRU runtime. This variation range is operationally justified, as the planned 1360 km transport distance is distributed over a two-day schedule, during which 20 hours are allocated to actual driving, allowing for plausible fluctuations due to traffic conditions and logistical delays. Results revealed a linear relationship, with

GWP increasing from 0.730 to 1.003 kg CO_2-eq, and a marginal sensitivity of 0.0014 kg CO_2-eq per kilometer (**Figure 9**). This confirms that transport logistics are a primary driver of cold chain climate impacts.

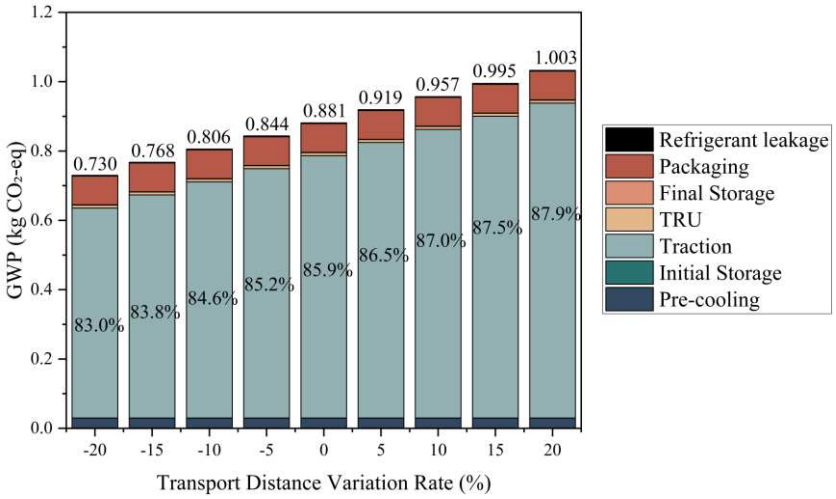

Figure 9 Sensitivity of GWP to transport distance variation in the baseline scenario.

The lifespan of RPC boxes was also varied to evaluate circularity benefits. Increasing reuse cycles from 560 to 840 trips yielded a modest reduction in GWP, with a marginal effect of -8.8×10^{-6} kg CO_2-eq per added use (**Figure 10**). Even with a ±20% change in the assumed RPC lifespan, the GWP contribution of RPC remained relatively minor, accounting for only 0.027%–0.041% of the total impact across the FCCL system. Although less influential than transport parameters, this outcome supports the promotion of reuse in cold chain infrastructure.

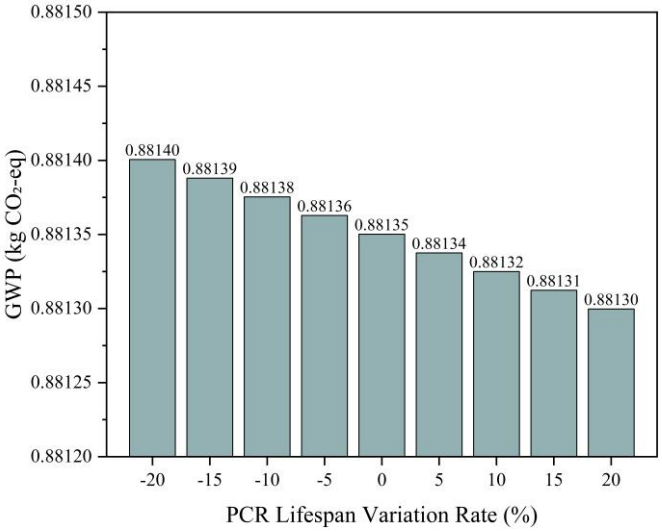

Figure 10 Sensitivity of GWP to RPC lifespan variation in the baseline scenario.

To evaluate uncertainty, a Monte Carlo simulation (n = 1000) was applied to the diesel-to-electricity efficiency of the TRU generator. This parameter followed a triangular distribution (minimum 35%, mode 42.75%, maximum 50%). The resulting GWP distribution for the baseline scenario had a mean of 0.864 kg CO_2-eq and a coefficient of variation of 4.39% (**Figure 11**). Although TRU efficiency contributes greater variability than most refrigeration pauses CCIs (which alter GWP by less than 0.05%), the relative performance ranking among scenarios remained stable, confirming the robustness of comparative outcomes.

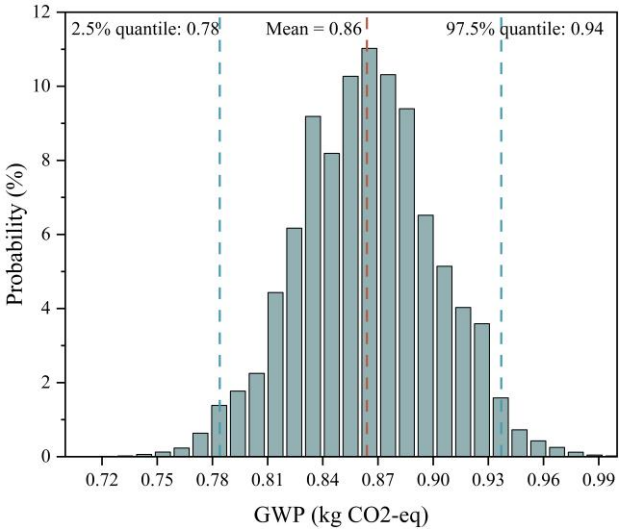

Figure 11 Uncertainty distribution of GWP due to TRU generator efficiency variation (n= 1000).

In addition, a comparative scenario was modeled to evaluate the climate mitigation potential of partial biodiesel substitution. B5 biodiesel, promoted in China, contains approximately 5% Fatty Acid Methyl Esters (FAME) derived from waste oils blended with fossil diesel (Hu et al., 2025). Replacing conventional diesel with B5 in the refrigerated truck subsystem led to measurable impact reductions: GWP decreased by 3.95%, HnCTP by 4.0%, FRSP by 4.2%, and PMFP by 2.7%. These results suggest that improving vehicle efficiency and adopting environmentally friendly fuels can deliver substantial environmental benefits across the FCCL without requiring major infrastructure changes.

4 Conclusion

This study proposes an integrated CFD–LCA framework to quantify the environmental impacts of CCIs during FCCL, within the defined boundaries, excluding

the upstream processes of cultivation and harvesting as well as the downstream consumption phase. By reconstructing dynamic temperature profiles under various interruption scenarios and converting them into energy demands and life cycle emissions, the method enables scenario-specific environmental assessments under non-steady-state conditions. It addresses the persistent gap between thermal dynamics and environmental modeling in cold chains, offering decision support for operators, fleet managers, and policymakers navigating trade-offs between energy efficiency, resilience, and quality assurance.

The CFD–LCA method enhances temporal resolution and scenario specificity by using physically grounded energy inputs derived from thermal simulations. It is suitable for assessing alternative packaging, staging strategies, or recovery protocols. The ability to simulate the full thermodynamic and environmental consequences of CCIs offers a valuable platform for optimizing logistics under uncertainty.

Simulation results show that these trade-offs are both nontrivial and context dependent. For example, a short refrigeration pause (e.g., ICT) slightly reduces GHG emissions (−0.026% GWP), due to reduced diesel use without rebound cooling. In contrast, ambient exposure (particularly AEPC), can sharply increase environmental burdens, with GWP rising by up to 5.94% (from 0.881 to 0.934 kg CO_2-eq/kg). This is driven by substantial thermal reabsorption and the intensified cooling loads in storage

and transport. Such findings highlight that conventional steady-state LCAs may underestimate the real-world climate costs of operational disruptions.

Quantitatively, the study reveals strong asymmetries in environmental sensitivity. IFS results in negligible variations across indicators (<0.001%), whereas ambient exposure, especially at early stages, could lead to disproportionate increases. In AEPC, the GWP of Initial Storage rises from 4.21×10^{-4} to 4.97×10^{-2} kg CO_2-eq, nearly two orders of magnitude greater than refrigeration pause scenarios. These results emphasize the importance of thermal continuity at transitions such as loading and handover, where even brief exposures can negate upstream cooling efforts and amplify downstream impacts.

It is important to note that the FCCL analyzed in this study represents only a part of the overall life cycle of the fresh product. If the environmental impacts from fruit cultivation, harvesting, supply chain waste and loss, as well as end-of-life treatments were included, the changes in the LCA results triggered by CCIs would be significantly reduced.

While this study focused on oranges, a relatively thermally resilient fruit, the proposed CFD-LCA integration framework is transferable to other perishable produce with appropriate parameter adjustments. For highly perishable items such as berries or leafy greens (Kroft et al., 2022; Zhou et al., 2022), the same modeling approach can be applied by adapting the thermal degradation kinetics and packaging configurations. In

these cases, even small thermal deviations can cause quality loss or spoilage, making the method particularly valuable for quantifying the environmental impacts of CCIs. Incorporating food waste flows in future studies would further enhance the completeness of environmental assessments.

The use of B5 biodiesel in transport ensured consistency across scenarios. However, future work should incorporate electric refrigerated trucks, which have demonstrated high GHG reduction potential, especially under low-carbon power grids. Including real-world electricity profiles, grid emission factors, and charging infrastructure would enable comprehensive comparisons between fossil-based and electric cold transport options.

Beyond retrospective analysis, the CFD–LCA approach holds potential for forward-looking optimization. Its temporal and physical resolution makes it well-suited for integration into digital twin systems or predictive logistics platforms, where scenario simulation can support adaptive decision-making (Shrivastava et al., 2022; Wu et al., 2023). For example, if a delay is detected, the model could evaluate route alternatives or refrigeration settings to minimize net emissions. This repositions LCA from a retrospective evaluator to a proactive planning tool, enhancing cold chain resilience in the face of operational variability and climate constraints.

Acknowledgements

This work was supported by the National Alternative Protein Innovation Centre (NAPIC), funded by Biotechnology and Biological Sciences Research Council (BBSRC) and Innovate UK [No. BB/Z516119/1], China Scholarship Council [No. 202406560019], and the Chang'an University High Performance Computing Platform. The authors would like to especially thank Prof. Nicholas Watson and Dr. Carl Gilkeson from the University of Leeds for their guidance on food quality and CFD modeling in this work. The authors gratefully acknowledge the financial and technical support provided by these organizations.

Reference

Armstrong, K., Dong, W., Jin, M., Nimbalkar, S., Cresko, J., 2025. Estimating energy consumption and GHG emissions in the U.S. food supply chain for net-zero. NPJ Sci Food 9, 1–16. https://doi.org/10.1038/S41538-024-00346-Y;SUBJMETA=1143,159,172,4000,4081,704,706;KWRD=AGRICULTURE,ECONOMICS,ENVIRONMENTAL+IMPACT

Baïri, A., 2014. Quantification of natural convective heat transfer within air-filled hemispherical cavities. Isothermal tilted disk with dome oriented upwards and wide Ra range. International Communications in Heat and Mass Transfer 57, 291–296. https://doi.org/10.1016/J.ICHEATMASSTRANSFER.2014.07.009

Bin, L., Jiawei, L., Aiqiang, C., Theodorakis, P.E., Zongsheng, Z., Jinzhe, Y., 2022. Selection of the cold logistics model based on the carbon footprint of fruits and vegetables in China. J Clean Prod 334, 130251. https://doi.org/10.1016/J.JCLEPRO.2021.130251

Ceballos-Santos, S., de Sousa, D.B., García, P.G., Laso, J., Margallo, M., Aldaco, R., 2024. Exploring the environmental impacts of plastic packaging: A comprehensive life cycle analysis for seafood distribution crates. Science of The Total Environment 951, 175452. https://doi.org/10.1016/J.SCITOTENV.2024.175452

Chen, Q., Qian, J., Yang, H., Li, J., Lin, X., Wang, B., 2024. Multiscale coupling analysis and modeling of airflow and heat transfer for warehouse-packaging-kiwifruit under forced-air cooling. Biosyst Eng 244, 166–176. https://doi.org/10.1016/J.BIOSYSTEMSENG.2024.06.007

Conradie, C.A., Goedhals-Gerber, L.L., van Dyk, F.E., 2022. Detecting temperature breaks in the initial stages of the citrus export cold chain: A case study. Journal of Transport and Supply Chain Management 16. https://doi.org/10.4102/JTSCM.V16I0.818

Corigliano, O., Algieri, A., 2024. A comprehensive investigation on energy consumptions, impacts, and challenges of the food industry. Energy Conversion and Management: X 23, 100661. https://doi.org/10.1016/J.ECMX.2024.100661

Cui, Q., Gao, E., Huang, S., Chen, M., Yu, H., Zhang, Z., Sun, Z., Jing, H., Zhang, X., 2025. Accounting and sensitivity analysis of CO2 emissions from typical food cold chain equipment in China. Environ Impact Assess Rev 113, 107881. https://doi.org/10.1016/J.EIAR.2025.107881

Daniel, L., 1∗, A., Jakhar, S., Dasgupta, M.S., 2024. Optimizing cold storage for uniform airflow and temperature distribution in apple preservation using CFD simulation. Scientific Reports 2024 14:1 14, 1–17. https://doi.org/10.1038/S41598-024-76385-Y

Dong, Y., Xu, M., Miller, S.A., 2020. Overview of cold chain development in china and methods of studying its environmental impacts. Environ Res Commun 2. https://doi.org/10.1088/2515-7620/ABD622

Duan, H., Song, G., Qu, S., Dong, X., Xu, M., 2019. Post-consumer packaging waste from express delivery in China. Resour Conserv Recycl 144, 137–143. https://doi.org/10.1016/J.RESCONREC.2019.01.037

Fabris, F., Artuso, P., Marinetti, S., Minetto, S., Rossetti, A., 2022. Cooling unit impact on energy and emissions of a refrigerated light truck. Appl Therm Eng 216, 119132. https://doi.org/10.1016/J.APPLTHERMALENG.2022.119132

Ferziger, J.H., Perić, M., Street, R.L., 2019. Computational Methods for Fluid Dynamics, Fourth Edition. Computational Methods for Fluid Dynamics 1–596. https://doi.org/10.1007/978-3-319-99693-6

Fitzgerald, W.B., Howitt, O.J.A., Smith, I.J., Hume, A., 2011. Energy use of integral refrigerated containers in maritime transportation. Energy Policy 39, 1885–1896. https://doi.org/10.1016/J.ENPOL.2010.12.015

Fu, M., Liu, H., Yang, W., Zhang, Q., Lv, Z., Nawaz, M., Jiao, Z., Liu, J., 2024. Virtual Cold Chain Method with Comprehensive Evaluation to Reveal the Effects of Temperature Abuse on Blueberry Quality. Foods 13, 3731. https://doi.org/10.3390/FOODS13233731

Gao, E., Cui, Q., Jing, H., Zhang, Z., Zhang, X., 2021. A review of application status and replacement progress of refrigerants in the Chinese cold chain industry. International Journal of Refrigeration 128, 104–117. https://doi.org/10.1016/J.IJREFRIG.2021.03.025

Gao, S., Yao, J., Zhao, X., Ren, P., Gustavsson, M., Wu, C., 2025. Review on life cycle analysis (LCA) studies of reusable plastic crates for fruit and vegetables. International Journal of Sustainable Engineering 18. https://doi.org/10.1080/19397038.2025.2457345

Goellner, K.N., Sparrow, E., 2014. An environmental impact comparison of single-use and reusable thermally controlled shipping containers. International Journal of Life Cycle Assessment 19, 611–619. https://doi.org/10.1007/S11367-013-0668-Z/FIGURES/7

Gruyters, W., Defraeye, T., Verboven, P., Berry, T., Ambaw, A., Opara, U.L., Nicolai, B., 2019. Reusable boxes for a beneficial apple cold chain: A precooling analysis. International Journal of Refrigeration 106, 338–349. https://doi.org/10.1016/J.IJREFRIG.2019.07.003

Guo, X., Yao, S., Wang, Q., Zhao, H., Zhao, Y., Zeng, F., Huo, L., Xing, H., Jiang, Y., Lv, Y., 2022. The impact of packaging recyclable ability on environment: Case and scenario analysis of polypropylene express boxes and corrugated cartons. Science of The Total Environment 822, 153650. https://doi.org/10.1016/J.SCITOTENV.2022.153650

Haque, M., Wang, B., Leandre Mvuyekure, A., Chaves, B.D., 2024. Validation of competition and dynamic models for Shiga toxin-producing Escherichia coli (STEC) growth in raw ground pork during temperature abuse. Food Microbiol 117, 104400. https://doi.org/10.1016/J.FM.2023.104400

Hu, Z., Shen, J., Tan, P., Lou, D., 2025. Life cycle carbon footprint of biodiesel production from waste cooking oil based on survey data in Shanghai, China. Energy 320, 135318. https://doi.org/10.1016/J.ENERGY.2025.135318

Huijbregts, M.A.J., Steinmann, Z.J.N., Elshout, P.M.F., Stam, G., Verones, F., Vieira, M., Zijp, M., Hollander, A., van Zelm, R., 2017. ReCiPe2016: a harmonised life cycle impact assessment method at midpoint and endpoint level. International Journal of Life Cycle Assessment 22, 138–147. https://doi.org/10.1007/S11367-016-1246-Y/TABLES/2

International Organization for Standardization, 2006. ISO 14040:2006 - Environmental management — Life cycle assessment — Principles and framework, 2nd ed. ISO.

IPCC, 2021. Climate Change 2021: The Physical Science Basis. Contribution of Working Group I to the Sixth Assessment Report of the Intergovernmental Panel on Climate Change. Cambridge University Press, Cambridge. https://doi.org/10.1017/9781009157896

IPCC, 2006. 2006 IPCC Guidelines for National Greenhouse Gas Inventories. Institute for Global Environmental Strategies (IGES) for the IPCC.

J. F. Thompson, D. C. Mejia, R. P. Singh, 2010. Energy Use of Commercial Forced-Air Coolers for Fruit. Appl Eng Agric 26, 919–924. https://doi.org/10.13031/2013.34934

Kroft, B., Gu, G., Bolten, S., Micallef, S.A., Luo, Y., Millner, P., Nou, X., 2022. Effects of temperature abuse on the growth and survival of Listeria monocytogenes on a wide variety of whole and fresh-cut fruits and vegetables during storage. Food Control 137, 108919. https://doi.org/10.1016/J.FOODCONT.2022.108919

Lin, H.J., Chen, P.C., Lin, H.P., Hsieh, I.Y.L., 2025. Quantifying carbon emissions in cold chain transport: A real-world data-driven approach. Transp Res D Transp Environ 142, 104679. https://doi.org/10.1016/J.TRD.2025.104679

Liu, G., Kuang, Z., Tang, J., Kuang, S., Tian, Q., Zou, Y., Li, Q., 2024. Calculation and utility analysis of lychee life-cycle carbon emissions considering food loss and waste. J Clean Prod 434, 140013. https://doi.org/10.1016/J.JCLEPRO.2023.140013

Lohita, B., Srijaya, M., 2024. Novel Technologies for Shelf-Life Extension of Food Products as a Competitive Advantage: A Review. Advances in Science, Technology and Innovation Part F2519, 285–306. https://doi.org/10.1007/978-3-031-51647-4_24/TABLES/1

Marchi, B., Bettoni, L., Zanoni, S., 2022. Assessment of Energy Efficiency Measures in Food Cold Supply Chains: A Dairy Industry Case Study. Energies (Basel) 15. https://doi.org/10.3390/EN15196901

Marques, C., Güneş, S., Vilela, A., Gomes, R., 2025. Life-Cycle Assessment in Agri-Food Systems and the Wine Industry—A Circular Economy Perspective. Foods 2025, Vol. 14, Page 1553 14, 1553. https://doi.org/10.3390/FOODS14091553

Meng, T., Wang, Yinpu, Fu, L., Wang, Yuelin, Zhang, N., Wang, Z., Yang, Q., 2023. Comparison of the environmental impact of typical packaging systems for food cold chain express based on life cycle assessment. J Clean Prod 139756. https://doi.org/10.1016/J.JCLEPRO.2023.139756

Ministry of Commerce of People's Republic of China (MOFCOM), 2021. China Renewable Resources Recycling Industry Development Report (2020).

Mustafa, M.F.M.S., Navaranjan, N., Demirovic, A., 2024. Food cold chain logistics and management: A review of current development and emerging trends. J Agric Food Res 18, 101343. https://doi.org/10.1016/J.JAFR.2024.101343

Neittaanmäki, P., Akimov, K., Akimova, V., Tuovinen, R., 2024. Challenges and Current Solutions of Refrigerated Transportation. Computational Methods in Applied Sciences 59, 241–256. https://doi.org/10.1007/978-3-031-61109-4_16/TABLES/1

Owoyemi, A., Holder, T., Porat, R., Lichter, A., Koenigstein, N., Salzer, Y., 2023. Temperature interruptions harm the quality of stored "Rustenburg" navel oranges and development of dynamic shelf-life prediction models. Postharvest Biol Technol 204, 112458. https://doi.org/10.1016/J.POSTHARVBIO.2023.112458

Rai, A., 2019. Energy demand and environmental impacts of food transport refrigeration and energy reduction methods during temperature-controlled distribution.

Shi, J., Li, T., Zhang, H., Peng, S., Liu, Z., Jiang, Q., 2015. Energy consummation and environmental emissions assessment of a refrigeration compressor based on life cycle assessment methodology. International Journal of Life Cycle Assessment 20, 947–956. https://doi.org/10.1007/S11367-015-0896-5

Shrivastava, C., Berry, T., Cronje, P., Schudel, S., Defraeye, T., 2022. Digital twins enable the quantification of the trade-offs in maintaining citrus quality and marketability in the refrigerated supply chain. Nat Food 3, 413–427. https://doi.org/10.1038/S43016-022-00497-9;SUBJMETA=1143,166,639,706,988;KWRD=AGRICULTURE,MECHANICAL+ENGINEERING

Skawińska, E., Zalewski, R.I., 2022. Economic Impact of Temperature Control during Food Transportation—A COVID-19 Perspective. Foods 2022, Vol. 11, Page 467 11, 467. https://doi.org/10.3390/FOODS11030467

Standardization Administration of the People's Republic of China (SAC), 2008. National Standard of Navel Orange. GB/T 21488-2008. General Administration of Quality Supervision, Inspection and Quarantine of the People's Republic of China (AQSIQ) and Standardization Administration of the People's Republic of China (SAC), Beijing.

Stellingwerf, H.M., Kanellopoulos, A., van der Vorst, J.G.A.J., Bloemhof, J.M., 2018. Reducing CO2 emissions in temperature-controlled road transportation using the LDVRP model. Transp Res D Transp Environ 58, 80–93. https://doi.org/10.1016/J.TRD.2017.11.008

Stoessel, F., Juraske, R., Pfister, S., Hellweg, S., 2012. Life cycle inventory and carbon and water foodprint of fruits and vegetables: Application to a swiss retailer. Environ Sci Technol 46, 3253–3262. https://doi.org/10.1021/ES2030577

Szpicer, A., Bińkowska, W., Wojtasik-Kalinowska, I., Salih, S.M., Półtorak, A., 2023. Application of computational fluid dynamics simulations in food industry. European Food Research and Technology 2023 249:6 249, 1411–1430. https://doi.org/10.1007/S00217-023-04231-Y

Tassou, S.A., De-Lille, G., Ge, Y.T., 2009. Food transport refrigeration – Approaches to reduce energy consumption and environmental impacts of road transport. Appl Therm Eng 29, 1467–1477. https://doi.org/10.1016/J.APPLTHERMALENG.2008.06.027

Tian, S., Wang, S., Xu, H., 2022. Early detection of freezing damage in oranges by online Vis/NIR transmission coupled with diameter correction method and deep 1D-CNN. Comput Electron Agric 193, 106638. https://doi.org/10.1016/J.COMPAG.2021.106638

UNEP and FAO, 2022. Sustainable food cold chains: Opportunities, challenges and the way forward, Sustainable food cold chains: Opportunities, challenges and the way forward. FAO, Nairobi, UNEP and Rome. https://doi.org/10.4060/CC0923EN

Waldhans, C., Albrecht, A., Ibald, R., Wollenweber, · Dirk, Sy, S.-J., Kreyenschmidt, J., 2024. Temperature Control and Data Exchange in Food Supply Chains: Current Situation and the Applicability of a Digitalized System of Time–Temperature-Indicators to Optimize Temperature Monitoring in Different Cold

Chains. Journal of Packaging Technology and Research 2024 8:1 8, 79–93. https://doi.org/10.1007/S41783-024-00165-2

Wang, X.F., Fan, Z.Y., Li, B.G., Liu, S., 2022. Forced-air cooling of iceberg lettuces: Cooling efficiency in relation to commercial operating strategies. International Journal of Refrigeration 139, 84–92. https://doi.org/10.1016/J.IJREFRIG.2022.04.010

Wu, J., Li, Q., Liu, G., Xie, R., Zou, Y., Scipioni, A., Manzardo, A., 2022a. Evaluating the impact of refrigerated transport trucks in China on climate change from the life cycle perspective. Environ Impact Assess Rev 97. https://doi.org/10.1016/J.EIAR.2022.106866

Wu, J., Liu, G., Marson, A., Fedele, A., Scipioni, A., Manzardo, A., 2022b. Mitigating environmental burden of the refrigerated transportation sector: Carbon footprint comparisons of commonly used refrigeration systems and alternative cold storage systems. J Clean Prod 372, 133514. https://doi.org/10.1016/J.JCLEPRO.2022.133514

Wu, W., Beretta, C., Cronje, P., Hellweg, S., Defraeye, T., 2019a. Environmental trade-offs in fresh-fruit cold chains by combining virtual cold chains with life cycle assessment. Appl Energy 254, 113586. https://doi.org/10.1016/J.APENERGY.2019.113586

Wu, W., Cronjé, P., Verboven, P., Defraeye, T., 2019b. Unveiling how ventilated packaging design and cold chain scenarios affect the cooling kinetics and fruit quality for each single citrus fruit in an entire pallet. Food Packag Shelf Life 21. https://doi.org/10.1016/J.FPSL.2019.100369

Wu, W., Häller, P., Cronjé, P., Defraeye, T., 2018. Full-scale experiments in forced-air precoolers for citrus fruit: Impact of packaging design and fruit size on cooling rate and heterogeneity. Biosyst Eng 169, 115–125. https://doi.org/10.1016/J.BIOSYSTEMSENG.2018.02.003

Wu, W., Shen, L., Zhao, Z., Harish, A.R., Zhong, R.Y., Huang, G.Q., 2023. Internet of Everything and Digital Twin enabled Service Platform for Cold Chain Logistics. J Ind Inf Integr 33, 100443. https://doi.org/10.1016/J.JII.2023.100443

Zhou, B., Luo, Y., Huang, L., Fonseca, J.M., Yan, H., Huang, J., 2022. Determining effects of temperature abuse timing on shelf life of RTE baby spinach through microbial growth models and its association with sensory quality. Food Control 133, 108639. https://doi.org/10.1016/J.FOODCONT.2021.108639